New Horizons in Earth Reinforcement – Otani, Miyata & Mukunoki (eds)
© 2008 Taylor & Francis Group, London, ISBN 978-0-415-45775-0

Parametric analysis of a 9-m high reinforced soil wall with different reinforcement materials and soil backfill

B. Huang
GeoEngineering Centre at Queen's-RMC, Department of Civil Engineering, Queen's University, Kingston, Ontario, Canada

K. Hatami
School of Civil Engineering and Environmental Science, University of Oklahoma, Norman, Oklahoma, USA

R.J. Bathurst
GeoEngineering Centre at Queen's-RMC, Department of Civil Engineering, Royal Military College of Canada, Kingston, Ontario, Canada

ABSTRACT: A verified FLAC model is used to investigate the influence of three different soil materials in combination with three different reinforcement materials on the behavior of otherwise identical modular block walls 9 m in height. The soils are a high quality sand backfill and two lower-quality c-ϕ materials. The reinforcement properties correspond to a uniaxial HDPE geogrid, a woven polyester geogrid and a welded wire mesh reinforcement product. The numerical results demonstrate the combined influence of reinforcement stiffness and soil mechanical properties on wall response. The numerical results show that for the same reinforcement type the largest deformations occurred when soil parameters corresponding to a CL backfill soil were assumed. However, the quantitative behavior of walls with ML soil properties and the nominal identical walls built with well-graded sand were similar with respect to wall deformations and reinforcement loads.

1 INTRODUCTION

A series of 11 full-scale instrumented reinforced soil walls has recently been completed at the Royal Military College of Canada (RMC). The test walls were 3.6 m in height. Most were constructed with solid modular block (segmental) facing units placed at a target batter of 8 degrees from the vertical. The walls were 3.3 m wide and the backfill extended about 6 m from the wall toe. The soil in each test was a high quality washed sand. The reinforcement materials were a uniaxial punched and drawn high density polyethylene (HDPE) geogrid, a woven polyester (PET) geogrid and a welded wire mesh (WWM) material. Some walls were constructed with different numbers of reinforcement layers, different facing batters and a wrapped-face configuration. Examples of two recent walls have been reported by Bathurst et al. (2006).

One objective of the physical test program was to generate a comprehensive set of physical test data that can be used to verify numerical codes. These codes can be used in turn to extend the physical test program to reinforced soil wall structures with a wider range of reinforcement materials, reinforcement spacing and length, different soils, facing types and batter angles. The measured results of four RMC walls were used to verify a numerical model using the program FLAC (Hatami & Bathurst 2005, 2006). A unique feature of the verification exercise was that a wide range of measured wall performance was compared to predicted values. These included wall deformations, footing loads, foundation pressures, reinforcement strains and connection loads.

In this paper an updated version of the FLAC code is now used to investigate the influence of three different soil materials on the behavior of nominally identical walls to the 3.6-m high RMC walls with a modular block facing, but extended to a wall height of 9 m. The soils were taken as a high quality sand backfill and two lower-quality c-ϕ soils. Three different reinforcement materials are used in the simulations.

2 NUMERICAL MODELS

2.1 *General*

The numerical simulations were carried out using the computer program FLAC (Itasca 2005). Sequential bottom-up construction of each segmental wall model and compaction of the soil was numerically simulated

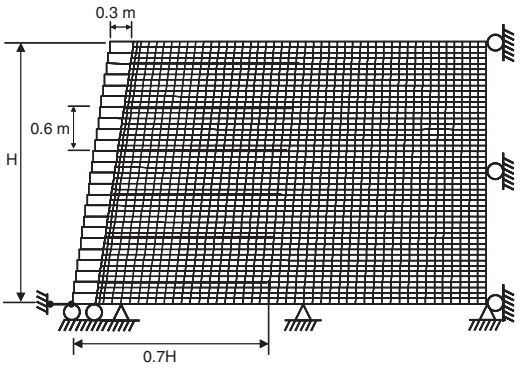

Figure 1. Typical FLAC numerical mesh.

following the procedures described by Hatami & Bathurst (2005). Computations were carried out in large-strain mode to ensure sufficient accuracy in the event of large wall deformations or reinforcement strains and to accommodate the moving local datum as each row of facing units and soil layer was placed during construction simulation. The same reinforcement length to height ratio of 0.7 was used in the numerical models. Similarly, the height of wall to length of soil mass in the cross-plane strain direction was kept the same as the original RMC physical wall models (Figure 1).

2.2 *Materials*

The compacted backfill soil was assumed as a homogenous, isotropic, nonlinear elastic material using the Duncan-Chang hyperbolic model. The elastic tangent modulus is expressed as:

$$E_t = \left[1 - \frac{R_f\left(1-\sin\phi\right)\left(\sigma_1-\sigma_3\right)}{2c\cos\phi + 2\sigma_3\sin\phi}\right]^2 K_e p_a \left(\frac{\sigma_3}{p_a}\right)^n \qquad (1)$$

where: σ_3 = minor principle stress, p_a = atmospheric pressure and other parameters are defined in Table 1. The original Duncan-Chang model was developed for axi-symmetric (triaxial) loading conditions. However, the boundary conditions for the RMC experimental walls, and for most walls in the field are closer to plane strain conditions. Hatami & Bathurst (2005) showed that the Duncan-Chang parameters back-fitted from triaxial tests on the RMC sand under-estimated the stiffness and strength of the same soil when tested in a plane strain test apparatus. This discrepancy is believed to be due to under-estimation of the average confining pressure of the soil specimens using the original Duncan-Chang formulation for bulk modulus, which is a function only of σ_3, specifically:

$$B = K_b p_a \left(\frac{\sigma_3}{p_a}\right)^m \qquad (2)$$

Table 1. Soil properties.

Property	Soil Type SW	ML	CL
K_e (elastic modulus number)	950	440	120
K_{ur} (unloading-reloading modulus number)[1]	1140	528	144
n (elastic modulus exponent)	0.60	0.40	0.45
R_f (failure ratio)	0.70	0.95	1.00
ν_t (tangent Poisson's ratio)	0–0.49	0–0.49	0–0.49
ϕ (friction angle) (degrees)[2]	48	37	17
c (cohesion) (kPa)	2	28	62
B_i/p_a (initial bulk modulus number)	74.8	48.3	21.2
ε_u (asymptotic volumetric strain value)	0.02	0.06	0.13
ρ (kg/m^3) (density)	2250	2030	1900

[1] $K_{ur} = 1.1 \times K_e$; [2] increased from peak triaxial values increased by 10% to adjust to peak plane strain values.

Hatami and Bathurst increased the value of parameter K_e by a factor of two in order to achieve satisfactory agreement with the plane strain test results. In the current study, the bulk modulus formulation proposed by Boscardin et al. (1990) was shown to give accurate predictions of plane strain test results for the RMC sand without using a multiplier applied to the elastic modulus number. The bulk modulus is expressed as:

$$B_t = B_i\left[1 + \frac{\sigma_m}{B_i\varepsilon_u}\right]^2 \qquad (3)$$

where: σ_m = mean pressure = $(\sigma_1 + \sigma_2 + \sigma_3)/3$; B_i and ε_u are material properties that are determined as the intercept and the inverse of slope from a plot of $\sigma_m/\varepsilon_{vol}$ versus σ_m in an isotropic compression test. An additional correction to triaxial test results was to increase the peak friction angle by 10% to reflect plane strain conditions.

Soil properties are summarized in Table 1. These parameters have been taken from Boscardin et al. (1990) with some adjustments. They represent soils with a wide range of mechanical properties. The highest quality soil designated as SW using the Unified Soil Classification System is a sand material. The lowest quality material is the CL soil. However, it is important to note that we are focused on the influence of mechanical strength and stiffness properties. Clearly, the CL soil is a less desirable backfill material from the point of view of ease of compaction, creep and potential loss of strength due to increases in moisture content.

Example stress-strain plots for the backfill soils used in this study are presented in Figure 2. Typical of non-linear elastic hyperbolic models of the type

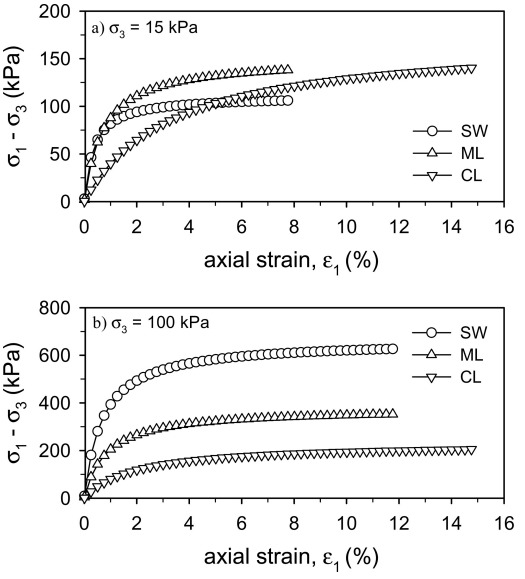

Figure 2. Computed example triaxial compression test results using soil parameters in Table 1.

discussed above, there is no strain-softening behavior. It should be noted that the focus of this paper is on the prediction of wall performance under operational conditions (i.e. working stress conditions). Hence, accurate modeling of the post-peak shear behavior of the soil backfill that can be expected to occur at incipient wall collapse is not a concern. Provided that strains in the reinforcement and soil remain low, the simple constitutive soil model used here is useful. This has been demonstrated in the verification studies reported by Hatami and Bathurst who successfully modeled the RMC walls that used a sand backfill up to reinforcement strain levels as great as 3%. Allen et al. (2003) reviewed a large number of monitored reinforced soil walls with granular backfills and concluded that contiguous failure zones and other obvious signs of poor wall performance did not occur if polymeric reinforcement strain levels were kept to less than about 3%. For cohesive soils, strain hardening can be expected to occur up to much larger strains. Miyata and Bathurst (2007) investigated the performance of monitored reinforced soil walls with c-ϕ backfill soils and noted that good performance was observed when reinforcement strains remained less than 4%. These reinforcement strain levels are benchmark values that can be used as indicators of the onset of contiguous zones of plasticity in numerical models. Hence, they can also be used to establish limits on the confidence that can be placed on numerical results generated using the constitutive soil model employed here.

Three different reinforcement materials were used to represent a range of materials with different

Table 2. Reinforcement properties.

Reinforcement type	Equation 4 and t = 1000 hours J_o (t) (kN/m)	η(t)	T_f (t) (kN/m)	Ultimate (index) strength $T_y^{(1)}$ (kN/m)
PET	285	0	NA	80
HDPE	1650	0.89	32.5	72
WWM	9300	0	NA	42

Notes: [1] Based on peak strength measured during 10% strain/minute constant-rate-of-strain (CRS) test; NA = not applicable for PET and WWM case with $\eta(t) = 0$.

load-strain-time characteristics and overall stiffness. The stiffness and strength properties for the PET and WWM have been scaled up from the material properties used in the original RMC physical tests and simulations reported by Hatami & Bathurst (2006).

A generalized time-dependent reinforcement tangent stiffness function $J_t(\varepsilon, t)$ proposed by Hatami & Bathurst (2006) was used to characterize the load-strain-time properties of the reinforcement materials:

$$J_t(\varepsilon,t) = \frac{1}{J_o(t)\left(\frac{1}{J_o(t)} + \frac{\eta(t)}{T_f(t)}\varepsilon\right)^2} \quad (4)$$

where: $J_o(t)$ is the initial tangent stiffness, $\eta(t)$ is a scaling function, $T_f(t)$ is the stress-rupture function for the reinforcement and, t is time. The values assumed in this study are given in Table 2 and correspond to a duration of loading of 1000 hours which is a reasonable elapsed time for a typical reinforced soil wall to come to equilibrium from start of construction (Allen et al. 2003). The relative stiffness of the reinforcement materials increases in the order of PET, HDPE and WWM in this investigation and varies by a factor of 30.

2.3 *Boundary conditions*

The interfaces between dissimilar materials were modelled as linear spring-slider systems with interface shear strength defined by the Mohr-Coulomb failure criterion. Direct shear tests were carried out on the solid masonry blocks used in the reference RMC experimental walls. The value of interface stiffness between modular blocks was selected to match the direct shear test results.

A fixed boundary condition in the horizontal direction was assumed at the numerical grid points on the backfill far-end boundary, representing the bulkheads that were used to contain the soil at the back of the RMC test facility. A fixed boundary condition in both horizontal and vertical directions was used at the foundation level matching the test facility concrete strong

Table 3. Interface properties.

Interface	Value
Soil-Block	
δ_{sb} (friction angle) (degrees)	48, 37, 17*
c_{sb} (cohesion) (kPa)	2, 28, 62*
ψ_{sb} (dilation angle) (degrees)	6, 2, 0
K_{nsb} (normal stiffness) (MN/m/m)	100
K_{ssb} (shear stiffness) (MN/m/m)	1
Block-Block	
δ_{bb} (friction angle) (degrees)	57
c_{bb} (cohesion) (kPa)	46
K_{nbb} (normal stiffness) (MN/m/m)	1000
K_{sbb} (shear stiffness) (MN/m/m)	40
Backfill-Reinforcement	
ϕ_b (friction angle) (degrees)	48, 37, 17*
s_b (adhesive strength) (kPa)	1000
K_b (shear stiffness) (kN/m/m)	1000

*Assumed equal to the friction angle of the backfill soil

floor. The toe of the facing column was restrained horizontally by a very stiff spring element with properties matching those measured at this boundary in the RMC physical tests. Interface properties are summarized in Table 3. The reinforcement-backfill interface properties were selected to prevent slip. There is no information available at present to select suitable quantitative values for any combination of reinforcement and soil. However, experience with the high quality sand used at RMC and measured reinforcement displacements suggests that this is a reasonable assumption for these conditions. In order to keep the interpretation of results as simple as possible, the same no-slip interface was considered for the c-ϕ soil cases in this numerical study. The reader is directed to the paper by Hatami & Bathurst (2005) for details of how the remaining interface material properties were selected.

3 EXAMPLE RESULTS

Figure 3 shows the out-of-alignment wall profiles at the end of construction. The horizontal datum at each elevation is the location of the wall if the facing blocks could be placed at the target 8-degree batter from the vertical without any movement. The data in Figures 3a, 3b and 3c show that the relative qualitative trends in the three profiles in each figure are similar. However, average quantitative deformations are less in the order of PET, HDPE and WWM (i.e. average deformations decrease with increasing reinforcement stiffness). However, at the top of the wall the maximum deformations are independent of reinforcement type. The explanation for this is that the soil controls wall deformation under working stress conditions (i.e. low reinforcement strain levels). The profiles shown here should not be confused with the relative displacement

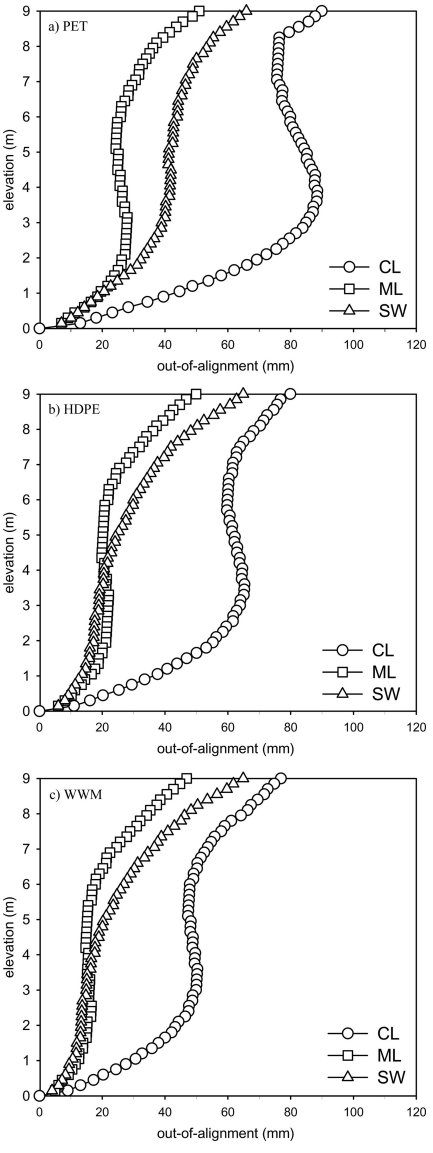

Figure 3. Out-of-alignment wall profiles at end of construction.

of the wall, which is the wall profile that is created when the relative movement of the block is measured from the time of installation. One example is illustrated in Figure 4. The shape of these plots was the same for all three reinforcement materials with most of the relative movement occurred over the bottom third of the wall height. Maximum relative displacements are summarized in Table 4b.

Figure 5 shows plots of connection and horizontal toe loads recorded for each wall at the end of

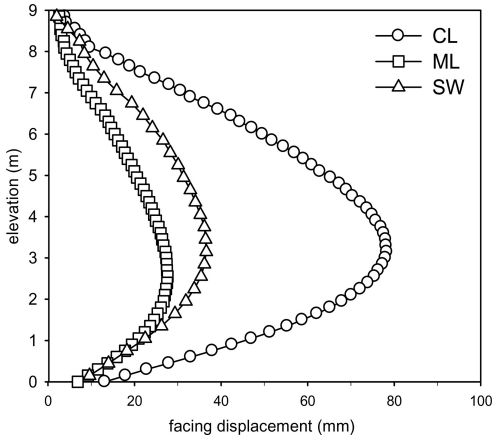

Figure 4. Relative facing displacement (PET reinforcement).

construction. For the polymeric reinforcement cases there are small but detectable lower reinforcement loads for the lower stiffness PET geogrid case compared to the HDPE case. The stiffer WWM wall generated the highest connection loads. The polymeric reinforcement cases show a more uniform distribution of loads while the stiffer metallic reinforcement cases show a trend of increasing load with depth below the top of the wall. Maximum connection loads and horizontal toe loads are summarized in Tables 4c and 4d, respectively. It can be seen in both Figure 5 and the tabulated results that there are significant toe loads generated at the base of the modular block facing as a result of the near-rigid horizontal boundary at this location. For the relatively extensible polymeric reinforcement cases the connection loads are about 30 to 60% of the total horizontal load summed over all connections and the restrained toe (Table 4e). For the stiffer WWM cases the connections loads range from 70 to 80% of the sum of total horizontal loads.

Example relative distributions of reinforcement loads (or strains) from numerical simulations are shown in Figure 6 as bar graphs along each reinforcement layer. For the case of a polymeric reinforcement material, Figure 6a shows that in general, the largest loads in the reinforcement occur at the connections. This is attributed to the effect of relative vertical settlement of the backfill soil with respect to the facing column, which becomes more pronounced with height above the toe. Figure 6b shows the same data but for a WWM reinforced soil wall case. It can be noted that the reinforcement loads are slightly more uniform and propagate deeper into the reinforced soil zone at the lower elevations. This can be attributed to the greater stiffer of the metallic reinforcement. The maximum strains in the reinforcement layers are summarized in Table 4f. The maximum strain levels for

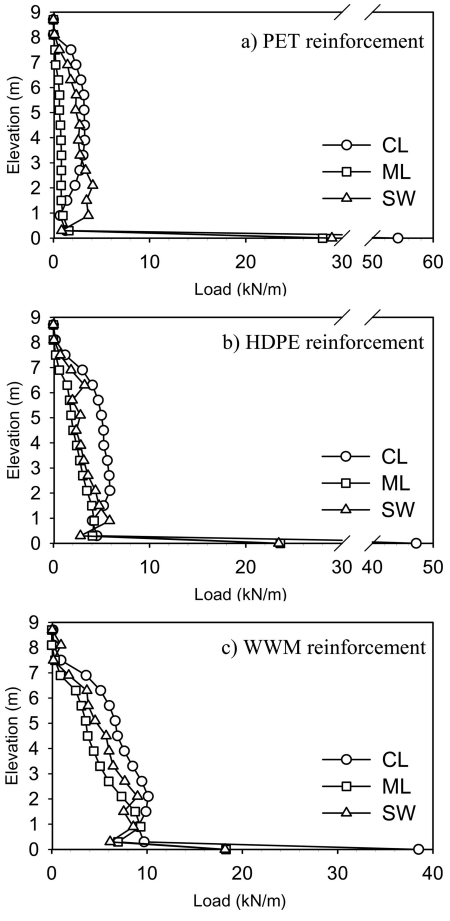

Figure 5. Connection and horizontal toe loads.

the polymeric reinforcement cases are consistent with working stress conditions as discussed in Section 2.2. The maximum strain in the metallic reinforcement is well within the yield strain limit of this reinforcement material (Hatami & Bathurst 2006).

4 CONCLUSIONS

A numerical parametric study is reported for three different soil types and three different reinforcement materials used in the construction of otherwise identical 9-m high modular block retaining walls. The numerical results show that for the same reinforcement type the largest deformations occurred when soil parameters corresponding to a CL backfill soil were assumed. However, the quantitative behavior of walls with ML soil and well-graded sand were similar with respect to wall deformations and reinforcement loads. These results show that a c-ϕ soil with the equivalent

Table 4. Results of numerical simulations.

Reinforcement	Soil type CL	ML	SW
a) maximum out-of-alignment (mm)			
PET	90	51	66
HDPE	80	50	65
WWM	77	47	65
b) maximum relative facing movement (mm)			
PET	78	29	37
HDPE	58	23	16
WWM	46	17	13
c) maximum connection loads (kN/m)			
PET	3.3	1.6	4.1
HDPE	5.9	4.2	5.8
WWM	10.1	9.3	9.0
d) horizontal toe loads (kN/m)			
PET	85.6	37.6	61.2
HDPE	106.9	55.6	63.9
WWM	132.6	80.5	90.5
e) ratio of sum of connection loads to sum of connection loads plus horizontal toe load (%)			
PET	37	26	53
HDPE	56	58	63
WWM	71	77	80
f) maximum reinforcement strains (%)			
PET	1.14	0.56	1.54
HDPE	0.50	0.30	0.36
WWM	0.15	0.11	0.11

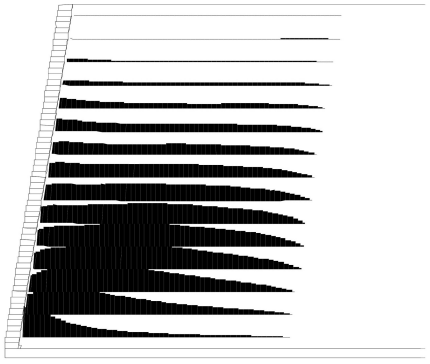

a) PET reinforcement with ML backfill soil (maximum strain = 0.56%).

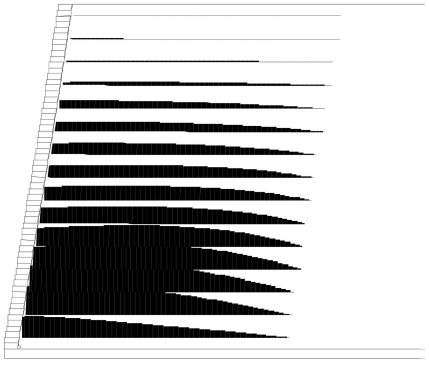

b) WWM reinforcement with ML backfill soil (maximum strain = 0.11 %)

Figure 6. Example distributions of reinforcement load.

mechanical properties of the ML soil in this study, can result in the same quantitatively good performance as a wall built with a purely frictional sand soil. Walls with relatively inextensible (metallic) reinforcement resulted in good performance in all cases but the magnitude and distribution of wall deformations and reinforcement loads were different from the structures with polymeric reinforcement.

Finally, while the performance of the wall models with the weakest and most compressible soil used in this investigation can be judged to have given satisfactory performance, it is important that walls with c-ϕ soils be carefully constructed and compacted, protected from surface water accumulation, and internally well drained so that the mechanical properties of the backfill are not allowed to degrade.

REFERENCES

Allen, T.M., Bathurst, R.J., Holtz, R.D., Walters, D.L. & Lee, W.F. 2003. A new working stress method for prediction of reinforcement loads in geosynthetic walls. *Canadian Geotechnical Journal*, Vol. 40, pp. 976–994.

Boscardin, M.D., Selig, E.T., Lin, R.S. & Yang, G.R. 1990. Hyperbolic parameters for compacted soils. ASCE *Journal of Geotechnical Engineering*, Vol. 116, No. 1, pp. 343–375.

Bathurst, R.J., Vlachopoulos, N., Walters, D.L., Burgess, P.G. & Allen, T.M. 2006. The influence of facing rigidity on the performance of two geosynthetic reinforced soil retaining walls. *Canadian Geotechnical Journal*, Vol. 43, No. 12, pp. 1225–1137.

Hatami, K. & Bathurst, R.J. 2005. Development and verification of a numerical model for the analysis of geosynthetic reinforced soil segmental walls under working stress conditions. *Canadian Geotechnical Journal*, Vol. 42, No. 4, pp. 1066–1085

Hatami, K. & Bathurst, R.J. 2006. A numerical model for reinforced soil segmental walls under surcharge loading. ASCE *Journal of Geotechnical and Geoenvironmental Engineering*, Vol. 132, No. 6, pp. 673–684.

Itasca Consulting Group, 2005. FLAC: Fast Lagrangian Analysis of Continua, version 5.0. Itasca Consulting Group, Inc., Minneapolis, Minnesota, USA.

Miyata, Y. & Bathurst, R.J. 2007. Development of K-Stiffness method for geosynthetic reinforced soil walls constructed with c-ϕ soils. *Canadian Geotechnical Journal*, (in press).